

Quantum and Classical Effects in Sample Excitations by Electron Beams

F. Javier García de Abajo^{1, 2, *} and Valerio Di Giulio¹

¹*ICFO-Institut de Ciències Fotoniques, The Barcelona Institute of Science and Technology, 08860 Castelldefels (Barcelona), Spain*

²*ICREA-Institució Catalana de Recerca i Estudis Avançats, Passeig Lluís Companys 23, 08010 Barcelona, Spain*

(Dated: October 24, 2021)

The wave nature of elementary particles manifests through interference effects ranging from double-slit experiments to diffraction by periodic lattices. These are typical configurations used in electron microscopy to image materials with atomic resolution. Likewise, interference is intuitively expected to show up in the creation of sample excitations by electron beams, but surprisingly, the excitation probability by a single electron is independent of its wave function, apart from a classical average over the transversal beam density profile. In contrast, the probability for two pulsed electrons depends on their relative spatial arrangement, thus reflecting the quantum nature of their interactions. We derive first-principles analytical expressions that embody these results and have general applicability to arbitrarily shaped electrons and any type of electron-sample interaction. The present study clarifies current misunderstandings on the role of the electron wave function in inelastic scattering and provides simple intuitive rules to understand configurations of practical interest.

I. INTRODUCTION

Interference of matter waves constitutes a genuine example of quantum phenomena. This is extensively exploited in electron microscopy [1–8], as well as in photoemission [9], low-energy [10], and laser-induced [11] electron diffraction (PD, LEED, and LIED, respectively), where self-interference permits unveiling structural information of materials and molecules with sub-Ångstrom spatial resolution. Shaping and probing the electron wave function lies at the heart of these techniques, in which electrons are scattered elastically, and consequently, no sample excitations are probed.

Inelastically scattered electrons carry information on the excited states of the sample, which can be revealed by performing electron energy-loss spectroscopy (EELS) [1–4] and has proved useful to characterize optical and vibrational modes [5–7, 12–15], benefiting from recent advances in electron microscope instrumentation [13, 16]. Some of these excitations are released as cathodoluminescence (CL) photon emission, which allows us to explore mode symmetries and lifetimes [17–23]. Interestingly, by synchronizing the electron with external light pumping, time-resolved LEED [24], LIED [11], and photon-induced near-field electron microscopy (PINEM) [25–56] grant us access into sample dynamics, including the possibility of studying the nonlinear optical response at the nanoscale [57]. Additionally, high spectral resolution can be achieved through performing electron energy-gain spectroscopy (EEGS) by scanning the pumping light frequency [41, 58, 59].

The question whether the excitation efficiency can be

modulated by shaping the electron wave function has been recurrently addressed in several studies [5, 56, 60–64]. For single monochromatic electrons, nonretarded theory was used to show that the excitation probability reduces to that produced by a classical point charge, averaged over the intensity of the transversal beam profile [60]. This result was latter generalized to include retardation [5], while the predicted independence on transversal wave function was experimentally corroborated for Smith-Purcell radiation [62]. The dependence on the longitudinal wave function is not as clear, with a recent report [64] claiming excitation probabilities for single and multiple electron pulses that depend on it. We note that this prediction radically differs from the results here obtained from a fully quantum-mechanical treatment of the electron-sample system.

A dependence on transversal wave function can however be observed by collecting only a finite angular range of scattered electrons [5, 60]. Specifically, for electrons transmitted along the center of the Fourier plane in an electron microscope, wave function shaping was experimentally demonstrated to actively select plasmon losses of different symmetry in metallic nanowires [61]. A wave function dependence should also be observed for interaction with excited samples in which the excitation maintains some degree of phase coherence with respect to the electron wave function [63], as experimentally illustrated in double PINEM experiments when the second PINEM coupling is driven by the same laser used to modulate the electron in the first PINEM interaction [33].

In this Letter, we elucidate the role of the electron wave function in the excitation of sample modes for any type of interactions with matter, photons, and polaritons. We present first-principles analytical expressions for the excitation probability by single and multiple electrons with arbitrarily shaped wave functions, based on which we conclude that the excitation from single elec-

*Corresponding author:
javier.garcia@nanophotonics.es

trons can be described fully classically with independence of the electron wave function, apart from a trivial average over the transversal beam profile. In contrast, multiple electrons produce correlations between their respective wave functions, which enter through the electron probability densities, whereas phase information is completely erased. Crucially, these results follow from the nonrecoil approximation (i.e., the electron velocity can be considered to be constant during interaction), which accurately applies under common conditions in electron microscopy (small beam energy spread and excitation energies compared with the average electron energy).

II. LACK OF WAVE-FUNCTION DEPENDENCE FOR SINGLE ELECTRONS

We consider a free electron propagating in vacuum and interacting with arbitrarily shaped material structures. Without loss of generality, the wave function of this combined system can be decomposed as

$$|\psi(t)\rangle = \sum_{\mathbf{q}n} \alpha_{\mathbf{q}n}(t) e^{-i(\varepsilon_{\mathbf{q}} + \omega_n)t} |\mathbf{q}n\rangle \quad (1)$$

using a complete basis set of combined material and radiation states $|n\rangle$ of energy $\hbar\omega_n$ and electron plane-wave states $|\mathbf{q}\rangle$ of well-defined momentum $\hbar\mathbf{q}$ and energy $\hbar\varepsilon_{\mathbf{q}}$. The elements of this basis set are eigenstates of the noninteracting Hamiltonian \mathcal{H}_0 , so they satisfy $\mathcal{H}_0|\mathbf{q}n\rangle = \hbar(\varepsilon_{\mathbf{q}} + \omega_n)|\mathbf{q}n\rangle$. This description is valid as long as no bound states of the electrons are involved. Under typical conditions in electron microscopes, the states $|n\rangle$ describe excitations in the sample, including the emission of photons, but also undesired excitations in other parts of the microscope (e.g., phonons in the electron source). For simplicity, we assume the electron to be prepared in a pure state prior to interaction with the sample [i.e., $\alpha_{\mathbf{q}n}(-\infty) = \delta_{n0}\alpha_{\mathbf{q}}^0$ with n denoting the ground state of the universe excluding the electron, subject to the normalization condition $\sum_{\mathbf{q}} |\alpha_{\mathbf{q}}^0|^2 = 1$], in the understanding that those undesired excitations can be later accounted for by tracing over different incoherent realizations of the electron wave function in the beam.

By inserting the Eq. (1) into the Schrödinger equation $(\mathcal{H}_0 + \mathcal{H}_1)|\psi\rangle = i\hbar\partial_t|\psi\rangle$, where the Hamiltonian \mathcal{H}_1 describes electron-sample interaction in a general way, we find the equation of motion $i\hbar\dot{\alpha}_{\mathbf{q}n} = \sum_{\mathbf{q}'n'} e^{i(\varepsilon_{\mathbf{q}} - \varepsilon_{\mathbf{q}'} + \omega_n - \omega_{n'})t} \langle \mathbf{q}n | \mathcal{H}_1 | \mathbf{q}'n' \rangle \alpha_{\mathbf{q}'n'}$ for the expansion coefficients $\alpha_{\mathbf{q}n}$. Now, the results presented in this work are a consequence of the following two assumptions, which are well justified for typical excitations probed in electron microscopy [5]:

(i) *Weak coupling.* The electron interaction with the sample is sufficiently weak as to neglect higher-order corrections to the excitation probability beyond the first order. This allows us to rewrite the equation of motion as $i\hbar\dot{\alpha}_{\mathbf{q}n} = \sum_{\mathbf{q}'} e^{i(\varepsilon_{\mathbf{q}} - \varepsilon_{\mathbf{q}'} + \omega_n)t} \langle \mathbf{q}n | \mathcal{H}_1 | \mathbf{q}'0 \rangle \alpha_{\mathbf{q}'}^0$ (with

$\omega_0 = 0$), which can be integrated to write the solution

$$\alpha_{\mathbf{q}n}(\infty) = \frac{-2\pi i}{\hbar} \sum_{\mathbf{q}'} \delta(\varepsilon_{\mathbf{q}} - \varepsilon_{\mathbf{q}'} + \omega_n) \langle \mathbf{q}n | \mathcal{H}_1 | \mathbf{q}'0 \rangle \alpha_{\mathbf{q}'}^0 \quad (2)$$

for the wave function coefficients after interaction.

(ii) *Nonrecoil paraxial approximation.* Electron beams feature small divergence angle (\sim a few mrad) and energy spread compared with the mean electron energy (i.e., $\alpha_{\mathbf{q}n}$ is negligible unless $|\mathbf{q} - \mathbf{q}_0| \ll q_0$, where $\hbar\mathbf{q}_0$ is the central electron momentum). Additionally, interaction with the sample produces wave vector components also satisfying $|\mathbf{q} - \mathbf{q}_0| \ll q_0$. This allows us to write the electron frequency difference as

$$\varepsilon_{\mathbf{q}} - \varepsilon_{\mathbf{q}'} \approx \mathbf{v} \cdot (\mathbf{q} - \mathbf{q}'), \quad (3)$$

indicating that only momentum transfers parallel to the beam contribute to transfer energy to the sample [5].

Putting these elements together and using the real-space representation of the electron states $\langle \mathbf{r} | \mathbf{q} \rangle = V^{-1/2} e^{i\mathbf{q} \cdot \mathbf{r}}$ with quantization volume V in Eq. (2), we find that the probability that the single electron excites a sample mode n , expressed through the trace of scattered electron degrees of freedom $P_n^0 = \sum_{\mathbf{q}} |\alpha_{\mathbf{q}n}(\infty)|^2$, reduces to (see detailed derivation in Appendix A)

$$P_n^0 = \int d^3\mathbf{r} |\psi^0(\mathbf{r})|^2 |\beta_n(\mathbf{R})|^2 \quad (4)$$

where

$$\psi^0(\mathbf{r}) = V^{1/2} \int \frac{d^3\mathbf{q}}{(2\pi)^3} \alpha_{\mathbf{q}}^0 e^{i\mathbf{q} \cdot \mathbf{r}} \quad (5)$$

is the incident electron wave function,

$$\beta_n(\mathbf{R}) = \frac{1}{\hbar v} \int dz e^{-i\omega_n z/v} \langle 0 | \mathcal{H}_1(\mathbf{r}) | n \rangle \quad (6)$$

is an electron-sample coupling coefficient that depends on transversal coordinates $\mathbf{R} = (x, y)$, and we choose the beam direction along z . Incidentally, this definition of β_n coincides with previous studies in which \mathcal{H}_1 describes electron-light PINEM interaction and n refers to optical modes [52, 56].

We observe from Eq. (4) that the excitation probability loses the dependence on the electron wave function profile along the beam direction z , as this enters just through an integral of the electron density along that direction. Additionally, the dependence on transverse directions \mathbf{R} consists in a weighted average of the probability $|\beta_n(\mathbf{R})|^2$ over the transversal profile of the beam intensity.

III. WAVE-FUNCTION DEPENDENCE IN THE CORRELATION AMONG MULTIPLE ELECTRONS

The above analysis can be readily extended to a beam pulse consisting of N electrons with incident wave functions $\psi^j(\mathbf{r})$. The probability of exciting a sample mode n

then reduces to (see detailed derivation in Appendix B)

$$P_n^{\text{total}} = \sum_j \int d^3\mathbf{r} |\psi^j(\mathbf{r})|^2 |\beta_n(\mathbf{R})|^2 + \sum_{j \neq j'} Q_n^j Q_n^{j'*}, \quad (7)$$

where

$$Q_n^j = \int d^2\mathbf{R} M_n^j(\mathbf{R}) \beta_n(\mathbf{R}), \quad (8)$$

$$M_n^j(\mathbf{R}) = \int dz e^{i\omega_n z/v} |\psi^j(\mathbf{r})|^2. \quad (9)$$

The first term in Eq. (7) corresponds to the uncorrelated excitation produced by N independent electrons, each of them expressed as a weighted average over the electron density profile, just like for a single electron in Eq. (4). The second term accounts for two-electron correlations, in which the phase of the electron wave functions is also erased, but there is still a dependence through the Fourier transform of the probability density in Eq. (9).

IV. BUNCHED AND DILUTED ELECTRON LIMITS

The linearized energy difference assumed in the non-recoil approximation [Eq. (3)] allows us to write the incident electron wave function [see Eq. (1)] as $\langle \mathbf{r}, n = 0 | \psi(t \rightarrow -\infty) \rangle = e^{-i\mathbf{e}_0 t} \psi^0(\mathbf{R}, z - vt)$ with ψ^0 given by Eq. (5). For N electrons differing in their wave functions just in their arrival times $t_j = z_j/v$, we have $|\psi^j(\mathbf{r})|^2 = |\psi^0(\mathbf{R}, z - z_j)|^2$, so Eq. (7) reduces to

$$P_n^{\text{total}} = NP_n^0 + |Q_n^0|^2 \sum_{j \neq j'} e^{i\omega_n(z_j - z_j)/v} \quad (10)$$

with $Q_n^0 = \int d^3\mathbf{r} e^{i\omega_n z/v} |\psi^0(\mathbf{r})|^2 \beta_n(\mathbf{R})$ and P_n^0 given by Eq. (4). In addition, if all electron wave function displacements satisfy $|z_j - z_j| \ll v/\omega_n$, neglecting linear terms in N , the sum in Eq. (10) becomes $\approx N^2 |Q_n^0|^2$, which can reach high values for large N , an effect known as superradiance when n represents radiative modes. We note that this effect does not require electrons confined within a small distance compared with the excitation length v/ω_n : superradiance is thus predicted to also take place for extended electron wave functions, provided all electrons share the same probability density, apart from small longitudinal displacements compared with v/ω_n in all realizations of the experiment; however, the magnitude of Q_n^0 will obviously decrease when the electron extends over several v/ω_n periods. Of course, if the electron density is further confined within a small region compared with v/ω_n , we readily find $P_n^{\text{total}} \approx N^2 P_n^0$. Superradiance has been experimentally observed for bunched electrons over a wide range of frequencies [65, 66] and constitutes the basis of free-electron lasers [66–68].

In the opposite limit of randomly arriving electrons and displacements z_j spanning a large spatial interval

compared with v/ω_n (even for perfect lateral alignment), the sum in Eq. (10) averages out and we obtain $P_n^{\text{total}} = NP_n^0$, so correlation effects are washed out.

V. INTERACTION WITH LOCALIZED EXCITATIONS

For illustration purposes, we consider a laterally focused Gaussian electron wavepacket with probability density $|\psi^0(\mathbf{r})|^2 \approx \delta(\mathbf{R} - \mathbf{b}) e^{-z^2/\Delta^2}/\sqrt{\pi}\Delta$ interacting with a localized excitation of frequency ω_n and transition dipole \mathbf{p} oriented as shown in Fig. 1(a). The EELS probability is then described by a coupling coefficient that scales as [52] $\beta_0(\mathbf{R}) \propto \mathbf{p} \cdot \hat{\mathbf{R}}$ with the direction of \mathbf{R} . Using these expressions for a single electron arranged in the two-wavepacket configurations of Fig. 1(b,c), we find from Eq. (4) an excitation probability $P_n^0 = |\beta_n(\mathbf{b})|^2 \propto |\mathbf{p}|^2$ that is independent of wavepacket separation a (explicit calculations of single-electron EELS probabilities are extensively discussed in the literature [5–7]). In contrast, for two electrons with each of them in a different wavepacket, we find from Eqs. (7)–(9)

$$P_n^{\text{total}}/2P_n^0 = 1 \pm S \cos(\varphi), \quad (11)$$

where $\varphi = \omega_n a/v$, $S = e^{-\omega_n^2 \Delta^2/2v^2}$, and the + and – signs apply to the configurations of Figs. 1(b) and 1(c), respectively (see Appendix C). Interestingly, for two electrons with their wave functions equally shared among the two wavepackets, we also observe oscillations with double period in a as

$$P_n^{\text{total}}/2P_n^0 = 1 + S \cos^2(\varphi/2) \quad (12)$$

in the $a \gg \Delta$ limit for the configuration of Fig. 1(b) [and the same expression with cos replaced by sin for Fig. 1(c)], which corresponds to the situation considered in Eq. (10) for z_j independent of j and two electrons sharing the same wave function. In general, for N laterally focused electrons, each of them having a wave function that is periodically distributed among L wavepackets with separation a , we have $P_n^{\text{total}}/NP_n^0 = 1 + [(N-1)/L^2] S \sin^2(L\varphi/2)/\sin^2(\varphi/2)$ (see Appendix C), which presents a maximum excitation probability independent of the number of periods L .

VI. INTERFERENCE IN THE EMISSION OF PHOTONS AND POLARITONS

When the sample has lateral translational invariance, like in Fig. 2, the excited modes possess well-defined in-plane wave vector $\mathbf{k}_{n\parallel}$, so the coupling coefficient exhibits a simple spatial dependence, $\beta_n(\mathbf{R}) \propto \beta_n(0) e^{i\mathbf{k}_{n\parallel} \cdot \mathbf{R}}$. Proceeding in a similar way as above for Gaussian wavepackets, we find no dependence on wave function for single electrons, whereas for two electrons we obtain the

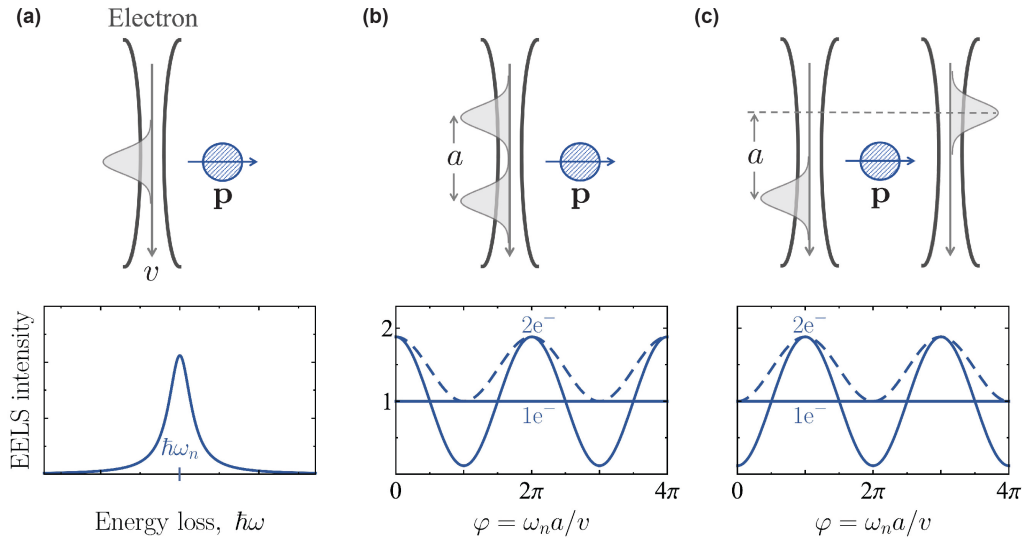


FIG. 1: **Interference in single- and double-electron interactions with a localized excitation.** (a) Sketch of an electron wavepacket interacting with a nanoparticle (top) and typical EELS spectrum (bottom) dominated by one resonance of frequency ω_n and polarization \mathbf{p} normal to the electron velocity \mathbf{v} . (b) Interaction with two electron wavepackets separated by a longitudinal distance a . If the wavepackets are part of a single-electron wave function, the EELS probability is independent of a ($1e^-$ solid curve). With two electrons, each of them in a different wavepacket, the EELS intensity oscillates with $\omega_n a / v$ and presents a maximum at $a = 0$ ($2e^-$ solid curve). For two electrons with their wave functions equally shared among the two wavepackets, the oscillations with a have double period ($2e^-$ dashed curve). (c) Interaction with two electron wavepackets in symmetrically arranged beams. We find similar results as in (b), but now the $2e^-$ probability displays a minimum at $a = 0$. We consider wavepackets of width given by $\omega_n \Delta / v = 0.5$. The EELS intensity is normalized to the result for uncorrelated electrons.

same results as in Eqs. (11) and (12) with ϕ redefined as $\omega_n a / v - \mathbf{k}_n \cdot \mathbf{b}$. The emission probability thus oscillates with both longitudinal and lateral wavepacket displacements, a and \mathbf{b} , respectively, as illustrated in Fig. 2.

VII. CONCLUDING REMARKS

When examining a sample excitation of frequency ω_n within a classical treatment of the electron as a point charge, the external source can be assimilated to a line charge with $e^{i\omega_n z/v}$ phase profile. The excitation strength by such classical charge distribution coincides with $|\beta_n(\mathbf{R})|^2$ [see Eq. (6)], where \mathbf{R} gives the transversal position of the line. Actually, summing over all final states to calculate the EELS probability $\sum_n |\beta_n|^2 \delta(\omega - \omega_n)$, we obtain a compact expression in terms of the electromagnetic Green tensor of the sample [69], which is widely used in practical simulations [5]. Extrapolating this classical picture to the configuration of Fig. 2, we consider two point electrons with lateral and longitudinal relative displacements, which directly yield an emission probability as described by Eq. (12). However, the classical picture breaks down for electrons whose wave functions are separated into several wavepackets: for single electrons, no classical interference between the emission from different wavepackets is observed, as the excitation probability reduces to a simple average of the line charge classical model over the transversal beam pro-

file; likewise, for multiple electrons the excitation probability depends on the electron wave function in a way that cannot be directly anticipated from the classical picture (cf. solid and dashed curves in Figs. 1 and 2).

The classical model provides an intuitive picture of interference in the CL emission from structured samples, such as in Smith-Purcell radiation [70] from periodic [71, 72], quasiperiodic [73], and focusing [74] gratings. In our formalism, the coherent properties of the emitted radiation are captured by the z integral in Eq. (6), where the matrix element of the interaction Hamiltonian reduces to the electric field associated with the excited mode [52]. In CL, the excited state n refers to a click in a photon detector, so the sample must be understood as a complex system composed by the structure probed in the microscope, the optical setup, and the detector itself.

We remark that the our results hold general applicability to any type of interaction Hamiltonian whose matrix elements $\langle n | \mathcal{H}_1(\mathbf{r}) | 0 \rangle$ are just a function of electron position \mathbf{r} [see Eq. (6)]. This includes arbitrarily complex materials and their excitations, as well as the coupling to any external field. In particular, the interaction with quantum electromagnetic fields is described by $\mathcal{H}_1 = (-1/c) \mathbf{A} \cdot \mathbf{j}$, where \mathbf{A} is the vector potential operator and \mathbf{j} is the electron current, which can be safely approximated by its classical value $-e\mathbf{v}$ in the nonrecoil approximation. Additionally, we treat the sample (i.e., the universe excluding the electron beam) as a close system, so its excitations are eigenstates of infinite lifetime.

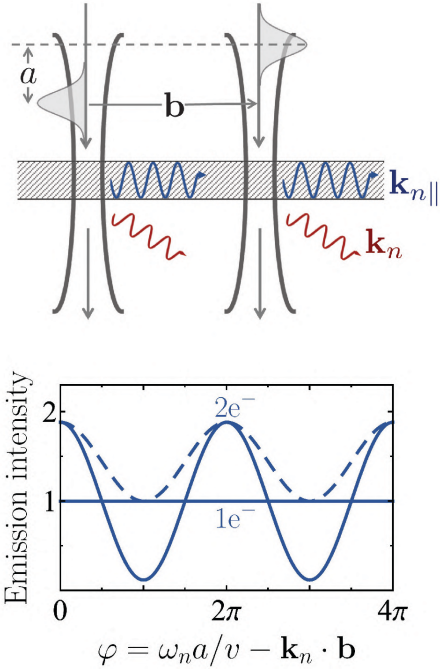


FIG. 2: **Interference in the interaction with delocalized modes.** For the two-wavepacket beam configuration of Fig. 1 and a sample that has lateral translational invariance, a single-electron of split wave function emits in-plane polaritons and transition radiation with an intensity that is insensitive to the longitudinal and lateral wavepacket separations a and b , in contrast to the emission intensity observed when each wavepacket has one electron ($2e^-$ solid curve) and when each electron occupies both wavepackets ($2e^-$ dashed curve). We use the same beam parameters as in Fig. 1.

In a more traditional treatment of the sample as an open system, our results can be directly applied to excitations of long lifetime compared with the electron pulse durations. Additionally, coupling to the continua of external modes can be incorporated through the Fano formalism [75] to produce, for example, spectral CL emission profiles from the probabilities obtained for the excitation of confined electronic systems (e.g., plasmonic nanoparticles).

Our work provides intuitive understanding of the role of the wave function in electron-beam inelastic scattering. The predicted effects could be experimentally corroborated from few-electron pulses produced for example by shaped laser pulses or multiple ionization from molecules. Besides its fundamental interest, the dependence on the wave function for multiple electrons opens the possibility of realising electron-electron pump-probe imaging with an ultimate time resolution fundamentally limited by the electron period $\sim \pi/vq_0 \sim 10^{-20}$ s for 100 keV electrons.

Acknowledgments

We thank Albert Polman, Ido Kaminer, Ofer Kfir, and Claus Ropers for helpful and enjoyable discussions. This work has been supported in part by ERC (Advanced Grant 789104-eNANO), the Spanish MINECO (MAT2017-88492-R and SEV2015-0522), the Catalan CERCA Program, and Fundació Privada Cellex. V.D.G. acknowledges financial support from the EU (Marie Skłodowska-Curie Grant 713729).

Appendix A: Derivation of Eqs. (4)-(6)

We calculate the excitation probability of sample mode n by tracing out over all final electron states as

$$P_n^0 = \sum_{\mathbf{q}} |\alpha_{\mathbf{q}n}(\infty)|^2 = \frac{(2\pi)^2}{\hbar^2} \sum_{\mathbf{q}} \left| \sum_{\mathbf{q}'} \delta(\varepsilon_{\mathbf{q}} - \varepsilon_{\mathbf{q}'} + \omega_n) \langle \mathbf{q}n | \mathcal{H}_1 | \mathbf{q}'0 \rangle \alpha_{\mathbf{q}'}^0 \right|^2, \quad (\text{A1})$$

where the rightmost expression is obtained by using Eq. (1). We now apply the prescription $\sum_{\mathbf{q}} \rightarrow V \int d^3 \mathbf{q} / (2\pi)^3$ to convert electron wave vector sums into integrals, adopt the nonrecoil approximation to write $\varepsilon_{\mathbf{q}} - \varepsilon_{\mathbf{q}'} = \mathbf{v} \cdot (\mathbf{q} - \mathbf{q}')$, and express the electron part of the matrix element in Eq. (A1) as a real-space integral, using the representation $\langle \mathbf{r} | \mathbf{q} \rangle = V^{-1/2} e^{i\mathbf{q} \cdot \mathbf{r}}$ for the electron momentum states. Then, choosing the $\hat{\mathbf{z}}$ axis along the electron velocity vector \mathbf{v} , we obtain

$$P_n^0 = \frac{V}{(2\pi)^7 \hbar^2 v^2} \int d^3 \mathbf{q} \left| \int d^3 \mathbf{q}' \delta(q_z - q'_z + \omega_n/v) \int d^3 \mathbf{r} e^{i(\mathbf{q}' - \mathbf{q}) \cdot \mathbf{r}} \langle n | \mathcal{H}_1(\mathbf{r}) | 0 \rangle \alpha_{\mathbf{q}'}^0 \right|^2.$$

We can use the δ function to perform the q'_z integral and then change the integration variable from q_z to $q_z + \omega_n/v$, so P_n^0 becomes

$$P_n^0 = \frac{V}{(2\pi)^7 \hbar^2 v^2} \int d^3 \mathbf{q} \left| \int d^2 \mathbf{R} e^{-i\mathbf{q}_{\perp} \cdot \mathbf{R}} \int d^2 \mathbf{q}'_{\perp} \alpha_{(\mathbf{q}'_{\perp}, q_z)}^0 e^{i\mathbf{q}'_{\perp} \cdot \mathbf{R}} \int dz e^{i\omega_n z/v} \langle n | \mathcal{H}_1(\mathbf{r}) | 0 \rangle \right|^2,$$

where we use the notation $\mathbf{r} = (\mathbf{R}, z)$ and $\mathbf{q} = (\mathbf{q}_{\perp}, q_z)$ with \mathbf{R} and \mathbf{q}_{\perp} standing for real and wave-vector coordinate components in the plane perpendicular to the beam direction. This expression can be simplified using the relation

$\int d^2\mathbf{q}_\perp \left| \int d^2\mathbf{R} e^{-i\mathbf{q}_\perp \cdot \mathbf{R}} f(\mathbf{R}) \right|^2 = (2\pi)^2 \int d^2\mathbf{R} |f(\mathbf{R})|^2$ and then changing \mathbf{q}'_\perp to \mathbf{q}_\perp . We find

$$P_n^0 = \frac{V}{(2\pi)^5 \hbar^2 v^2} \int d^2\mathbf{R} \left[\int dq_z \left| \int d^2\mathbf{q}_\perp \alpha_{\mathbf{q}}^0 e^{i\mathbf{q}_\perp \cdot \mathbf{R}} \right|^2 \right] \left[\left| \int dz e^{i\omega_n z/v} \langle n | \mathcal{H}_1(\mathbf{r}) | 0 \rangle \right|^2 \right].$$

Finally, using the identity $\int dq_z \left| \int d^2\mathbf{q}_\perp \alpha_{\mathbf{q}}^0 e^{i\mathbf{q}_\perp \cdot \mathbf{R}} \right|^2 = (2\pi)^{-1} \int dz \left| \int d^3\mathbf{q} \alpha_{\mathbf{q}}^0 e^{i\mathbf{q} \cdot \mathbf{r}} \right|^2$, we find the result

$$P_n^0 = \int d^3\mathbf{r} \left[\left| V^{1/2} \int \frac{d^3\mathbf{q}}{(2\pi)^3} \alpha_{\mathbf{q}}^0 e^{i\mathbf{q} \cdot \mathbf{r}} \right|^2 \right] \left[\left| \frac{1}{\hbar v} \int dz e^{-i\omega_n z/v} \langle 0 | \mathcal{H}_1(\mathbf{r}) | n \rangle \right|^2 \right] = \int d^3\mathbf{r} |\psi^0(\mathbf{r})|^2 |\beta_n(\mathbf{R})|^2, \quad (\text{A2})$$

which is Eq. (4), with $\psi^0(\mathbf{r})$ and $\beta_n(\mathbf{R})$ defined by Eqs. (5) and (6).

Appendix B: Derivation of Eqs. (6)-(9)

A direct extension of the general formalism used in Sec. A allows us to deal with N free electrons prepared in initial states (before interaction with the sample) described by their wave function coefficients $\alpha_{\mathbf{q}}^j$ with $j = 0, \dots, N-1$. The wave function of the combined system formed by the sample and the electrons can be written as

$$|\psi(t)\rangle = \sum_{\{\mathbf{q}\}n} \alpha_{\{\mathbf{q}\}n}(t) e^{-i(\sum_j \varepsilon_{\mathbf{q}_j} + \omega_n)t} |\{\mathbf{q}\}n\rangle,$$

where $\{\mathbf{q}\}$ denotes the ensemble of wave vectors \mathbf{q}_j . Given the large size of the electron configuration space in a microscope, we consider that it is safe to disregard for simplicity spin degrees of freedom and the Pauli exclusion principle. We further neglect electron-electron Coulomb interaction in the beam. Additionally, we work in the weak coupling regime, under the assumption that the sample is excited once at most by the passage of the N electrons, which is a good approximation with $N \ll 1/P_n^0$ for typical excitation probabilities $P_n^0 \sim 10^{-5}$ per electron for a single sample mode n . This allows us to integrate the Schrödinger equation to find the wave function coefficients after interaction as a generalization of Eq. (2):

$$\alpha_{\{\mathbf{q}\}n}(\infty) = \frac{-2\pi i}{\hbar} \sum_{\{\mathbf{q}'\}} \delta \left(\omega_n + \sum_j \varepsilon_{\mathbf{q}_j \mathbf{q}'_j} \right) \langle \{\mathbf{q}\}n | \mathcal{H}_1 | \{\mathbf{q}'\}0 \rangle \prod_j \alpha_{\mathbf{q}'_j}^j, \quad (\text{B1})$$

where $\varepsilon_{\mathbf{q}_j \mathbf{q}'_j} = \varepsilon_{\mathbf{q}_j} - \varepsilon_{\mathbf{q}'_j}$. Now, each of the terms in the real-space representation of the interaction Hamiltonian $\mathcal{H}_1(\mathbf{r}) = \sum_j \mathcal{H}_1(\mathbf{r}_j)$ depends on just one of the electron coordinates, and thus, because of the orthogonality of the electron momentum states, $\{\mathbf{q}\}$ and $\{\mathbf{q}'\}$ in Eq. (B1) differ by no more than one of the electron wave vectors. This allows us to recast this expression as

$$\alpha_{\{\mathbf{q}\}n}(\infty) = \frac{-2\pi i}{\hbar} \left(\prod_j \alpha_{\mathbf{q}_j}^j \right) \sum_j \sum_{\mathbf{q}'_j} \delta \left(\omega_n + \varepsilon_{\mathbf{q}_j \mathbf{q}'_j} \right) \langle \mathbf{q}_j n | \mathcal{H}_1 | \mathbf{q}'_j 0 \rangle \left(\alpha_{\mathbf{q}'_j}^j / \alpha_{\mathbf{q}_j}^j \right). \quad (\text{B2})$$

The excitation probability of sample mode n is obtained by tracing out the final electron states

$$P_n^{\text{total}} = \sum_{\{\mathbf{q}\}} |\alpha_{\{\mathbf{q}\}n}(\infty)|^2, \quad (\text{B3})$$

which, in combination with Eq. (B2) and the normalization condition of the initial states $\sum_{\mathbf{q}} |\alpha_{\mathbf{q}}^j|^2 = 1$, leads to

$$P_n^{\text{total}} = \sum_j P_n^j + \sum_{j \neq j'} Q_n^j Q_n^{j'*}, \quad (\text{B4})$$

where

$$P_n^j = \frac{(2\pi)^2}{\hbar^2} \sum_{\mathbf{q}_j} \left| \sum_{\mathbf{q}'_j} \delta \left(\varepsilon_{\mathbf{q}_j \mathbf{q}'_j} + \omega_n \right) \langle \mathbf{q}_j n | \mathcal{H}_1 | \mathbf{q}'_j 0 \rangle \alpha_{\mathbf{q}'_j}^j \right|^2 \quad (\text{B5})$$

and

$$Q_n^j = \frac{2\pi}{\hbar} \sum_{\mathbf{q}_j \mathbf{q}'_j} \delta\left(\varepsilon_{\mathbf{q}_j \mathbf{q}'_j} + \omega_n\right) \langle \mathbf{q}'_j 0 | \mathcal{H}_1 | \mathbf{q}_j n \rangle \alpha_{\mathbf{q}'_j}^{j*} \alpha_{\mathbf{q}_j}^j. \quad (\text{B6})$$

Noticing that Eq. (B5) is just like Eq. (A1) with $\alpha_{\mathbf{q}'}^0$ substituted by $\alpha_{\mathbf{q}'_j}^j$, we can write from Eq. (A2)

$$P_n^j = \int d^3 \mathbf{r} |\psi^j(\mathbf{r})|^2 |\beta_n(\mathbf{R})|^2 \quad (\text{B7})$$

with

$$\psi^j(\mathbf{r}) = V^{1/2} \int \frac{d^3 \mathbf{q}}{(2\pi)^3} \alpha_{\mathbf{q}}^j e^{i\mathbf{q} \cdot \mathbf{r}}. \quad (\text{B8})$$

Now, using the nonrecoil approximation $\varepsilon_{\mathbf{q}_j \mathbf{q}'_j} = v(q_{jz} - q'_{jz})$, transforming wave vector sums into integrals, expressing matrix elements as real-space integrals, and proceeding in a similar way as in the derivation of Eq. (A2) in Sec. A, we can rearrange Eq. (B6) as

$$\begin{aligned} Q_n^j &= \frac{V}{(2\pi)^5 \hbar v} \int d^3 \mathbf{q}_j \int d^3 \mathbf{q}'_j \int d^2 \mathbf{R} e^{i(\mathbf{q}_{j\perp} - \mathbf{q}'_{j\perp}) \cdot \mathbf{R}} \alpha_{\mathbf{q}_j}^{j*} \alpha_{\mathbf{q}_j}^j \delta(q_{jz} - q'_{jz} + \omega_n/v) \int dz e^{-i\omega_n z/v} \langle 0 | \mathcal{H}_1(\mathbf{r}) | n \rangle \\ &= \int d^2 \mathbf{R} M_n^j(\mathbf{R}) \beta_n(\mathbf{R}), \end{aligned} \quad (\text{B9})$$

where the coupling coefficient $\beta_n(\mathbf{R})$ is defined in Eq. (6), whereas

$$\begin{aligned} M_n^j(\mathbf{R}) &= \frac{V}{(2\pi)^5} \int d^3 \mathbf{q}_j \int d^3 \mathbf{q}'_j e^{i(\mathbf{q}_{j\perp} - \mathbf{q}'_{j\perp}) \cdot \mathbf{R}} \alpha_{\mathbf{q}_j}^j \alpha_{\mathbf{q}'_j}^{j*} \delta(q_{jz} - q'_{jz} + \omega_n/v) \\ &= \frac{V}{(2\pi)^5} \int d^3 \mathbf{q}_j \int d^3 \mathbf{q}'_j e^{i(\mathbf{q}_{j\perp} - \mathbf{q}'_{j\perp}) \cdot \mathbf{R}} \alpha_{\mathbf{q}_j}^j \alpha_{\mathbf{q}'_j}^{j*} \frac{1}{2\pi} \int dz e^{i(q_{jz} - q'_{jz} + \omega_n/v)z} \\ &= \int dz e^{i\omega_n z/v} \left[V^{1/2} \int \frac{d^3 \mathbf{q}_j}{(2\pi)^3} \alpha_{\mathbf{q}_j}^j e^{i\mathbf{q}_j \cdot \mathbf{r}} \right] \left[V^{1/2} \int \frac{d^3 \mathbf{q}'_j}{(2\pi)^3} \alpha_{\mathbf{q}'_j}^{j*} e^{-i\mathbf{q}'_j \cdot \mathbf{r}} \right] \\ &= \int dz e^{i\omega_n z/v} |\psi^j(\mathbf{r})|^2 \end{aligned}$$

becomes Eq. (9), the Fourier transform of the electron probability density in the incident electron wave function j .

Appendix C: Derivation of Eqs. (11) and (12)

We consider electron wave functions constructed in terms of normalized Gaussian wavepackets of the form $\psi_G(\mathbf{r}) = \psi_{\perp}(\mathbf{R}) e^{-z^2/2\Delta^2} / \pi^{1/4} \Delta^{1/2}$, where we factorize the transversal dependence in $\psi_{\perp}(\mathbf{R})$. For simplicity, we approximate $|\psi_{\perp}(\mathbf{R})|^2 \approx \delta(\mathbf{R})$ under the assumption that the transversal width w is small compared with the characteristic length of variation of the electric field associated with the excited mode n , or equivalently, $|\nabla_{\mathbf{R}} \beta_n(\mathbf{R})| \ll 1/w$. The configurations discussed in Figs. 1 and 2 involve electron wave functions of the general form

$$\psi^j(\mathbf{r}) = N_j^{-1} \sum_s \gamma_s^j \psi_G(\mathbf{r} - \mathbf{r}_s), \quad (\text{C1})$$

where we assume the same longitudinal wavepacket width Δ for all components, and $N_j = (\sum_{ss'} \gamma_s^j \gamma_{s'}^{j*} I_{ss'})^{1/2}$ is a normalization constant that depends on the overlap integrals

$$I_{ss'} = \begin{cases} (\sqrt{\pi} \Delta)^{-1} \int dz e^{-(z-z_s)^2/2\Delta^2} e^{-(z-z_{s'})^2/2\Delta^2} = e^{-(z_s - z_{s'})^2/4\Delta^2}, & \text{if } \mathbf{R}_s = \mathbf{R}_{s'}, \\ 0, & \text{otherwise.} \end{cases}$$

Plugging Eq. (C1) into Eqs. (B7) and (B9), we readily find

$$P_n^j = \frac{\sum_{ss'} \gamma_s^j \gamma_{s'}^{j*} I_{ss'} |\beta_n(\mathbf{R}_s)|^2}{\sum_{ss'} \gamma_s^j \gamma_{s'}^{j*} I_{ss'}} \approx \frac{\sum_s |\gamma_s^j|^2 |\beta_n(\mathbf{R}_s)|^2}{\sum_s |\gamma_s^j|^2}, \quad (\text{C2a})$$

$$Q_n^j = \sqrt{S} \frac{\sum_{ss'} \gamma_s^j \gamma_{s'}^{j*} I_{ss'} e^{i\omega(z_s + z_{s'})/2v} \beta_n(\mathbf{R}_s)}{\sum_{ss'} \gamma_s^j \gamma_{s'}^{j*} I_{ss'}} \approx \sqrt{S} \frac{\sum_s |\gamma_s^j|^2 e^{i\omega z_s/v} \beta_n(\mathbf{R}_s)}{\sum_s |\gamma_s^j|^2}, \quad (\text{C2b})$$

where

$$S = \left(\frac{1}{\sqrt{\pi}\Delta} \int dz e^{i\omega_n z/v} e^{-z^2/\Delta^2} \right)^2 = e^{-\omega_n^2 \Delta^2 / 2v^2}.$$

The rightmost approximations in Eqs. (C2) correspond to the nonoverlapping wavepacket limit (i.e., $|z_s - z_{s'}| \gg \Delta$ for $s \neq s'$), which yields $I_{ss'} = \delta_{s,s'}$. Now, we adopt this limit and specify Eqs. (B4) and (C2) for the beams studied in Figs. 1 and 2:

- Figure 1(b):
 - We consider two Gaussian wavepackets $s = 0, 1$ with longitudinal coordinates $z_0 = 0$ and $z_1 = a$, where a is the wavepacket separation, and the same lateral coordinates $\mathbf{R}_s = \mathbf{b}$, so $\beta_n(\mathbf{R}_s) = \beta_n(\mathbf{b})$ is independent of s and factors out in Eqs. (C2). In particular, Eq. (C2a) reduces to $P_n^j = |\beta_n(\mathbf{b})|^2$.
 - For two electrons $j = 0, 1$, each of them fully contained in one of the two wavepackets, we have $|\gamma_s^j|^2 = \delta_{s,j}$, so Eq. (C2b) gives $Q_n^0 = \sqrt{S}\beta_n(\mathbf{b})$ and $Q_n^1 = \sqrt{S}\beta_n(\mathbf{b})e^{i\omega_n a/v}$. Inserting these expressions in Eq. (B4), we find $P_n^{\text{total}} = 2|\beta_n(\mathbf{b})|^2 [1 + S \cos(\omega_n a/v)]$ [i.e., Eq. (11) with the + sign]. Incidentally, this result remains unchanged even when the wavepackets overlap.
 - If each of the two electrons is equally shared among the two wavepackets, we have $|\gamma_s^j|^2 = 1/2$. Evaluating Eq. (C2b) with these coefficients, we find $Q_n^0 = Q_n^1 = \sqrt{S}\beta_n(\mathbf{b})(1 + e^{i\omega_n a/v})/2$, which together with Eq. (B4) lead to the result $P_n^{\text{total}} = 2|\beta_n(\mathbf{b})|^2 [1 + S \cos^2(\omega_n a/2v)]$ [i.e., Eq. (12)].
- Figure 1(c):
 - We consider two wavepackets $s = 0, 1$ with $\mathbf{R}_0 = -\mathbf{R}_1 = \mathbf{b}$, $z_0 = 0$, and $z_1 = a$. Because $|\beta_n(\mathbf{R}_s)|$ is also independent of s (see below), we can factor it out in Eq. (C2a), which leads again to $P_n^j = |\beta_n(\mathbf{b})|^2$.
 - To describe two electrons, each of them separated in different wavepackets, we take $|\gamma_s^j|^2 = \delta_{s,j}$, so Eq. (C2b) gives $Q_n^0 = \sqrt{S}\beta_n(\mathbf{b})$ and $Q_n^1 = -\sqrt{S}\beta_n(\mathbf{b})e^{i\omega_n a/v}$, where we have used the property $\beta_n(-\mathbf{b}) = -\beta_n(\mathbf{b})$ for the coefficient of coupling to an excitation with the transition dipole oriented as shown in Fig. 1. We thus find from Eq. (B4) $P_n^{\text{total}} = 2|\beta_n(\mathbf{b})|^2 [1 - S \cos(\omega_n a/v)]$ [i.e., Eq. (11) with the - sign].
 - Proceeding as above for the configuration in which each of the two electrons is equally shared among the two wavepackets, we find $Q_n^0 = Q_n^1 = \sqrt{S}\beta_n(\mathbf{b})(1 - e^{i\omega_n a/v})/2$, which now results in $P_n^{\text{total}} = 2|\beta_n(\mathbf{b})|^2 [1 + S \sin^2(\omega_n a/2v)]$ [i.e., Eq. (12) with cos replaced by sin].
- Figure 2: In this configuration, the coupling coefficient has the same spatial periodicity as the excited mode [i.e., $\beta_n(\mathbf{R}_s) = \beta_n(0)e^{i\mathbf{k}_n \cdot \mathbf{R}_s}$ picks up the mode propagation phase at the region of electron-sample interaction]. With the same choice of wave function coefficients as in the above analysis of Fig. 1(c), and considering a lateral separation $\mathbf{b} = \mathbf{R}_0 - \mathbf{R}_1$ between the two wavepackets, we straightforwardly find the same expressions for the excitation probability, but with $\omega_n a/v$ replaced by $\omega_n a/v - \mathbf{k}_n \cdot \mathbf{b}$.

In the main text, we also discuss a generalization of Fig. 1(b) to a beam consisting of N electrons ($j = 0, \dots, N-1$) distributed among L periodically arranged wavepackets ($s = 0, \dots, L-1$) with longitudinal spacing a and the same lateral position $\mathbf{R}_s = \mathbf{b}$ for all. Proceeding in a similar way as in the above analysis of Fig. 1(b), we take $|\gamma_s^j|^2 = 1/L$ and find from Eqs. (C2) the results $P_n^j = |\beta_n(\mathbf{b})|^2$ and $Q_n^j = \sqrt{S} |\beta_n(\mathbf{b})|^2 (1/L) \sum_s e^{i\omega_n a/v}$, which combined with Eq. (C2) lead to $P_n^{\text{total}} = N |\beta_n(\mathbf{b})|^2 \{1 + [(N-1)/L^2] S \sin^2(L\omega_n a/2v) / \sin^2(\omega_n a/2v)\}$.

- [1] R. F. Egerton, *Electron Energy-Loss Spectroscopy in the Electron Microscope* (Plenum Press, New York, 1996).
- [2] R. F. Egerton, *Micron* **34**, 127 (2003).
- [3] R. Erni and N. D. Browning, *Ultramicroscopy* **104**, 176 (2005).
- [4] R. Brydson, *Electron Energy Loss Spectroscopy* (BIOS Scientific Publishers, Oxford, 2001).
- [5] F. J. García de Abajo, *Rev. Mod. Phys.* **82**, 209 (2010).
- [6] M. Kociak and O. Stéphan, *Chem. Soc. Rev.* **43**, 3865 (2014).
- [7] A. Polman, M. Kociak, and F. J. García de Abajo, *Nat. Mater.* **18**, 1158 (2019).
- [8] E. Bauer, *Rep. Prog. Phys.* **57**, 895 (1994).
- [9] C. S. Fadley, *J. Electron Spectros. Relat. Phenomena*

178-179, 2 (2010).

[10] J. B. Pendry, in *Determination of Surface Structure by LEED*, edited by P. M. Marcus and F. Jona (Plenum Press, New York, 1984), p. 3.

[11] B. Wolter, M. G. Pullen, A.-T. Le, M. Baudisch, K. Doblhoff-Dier, A. Senftleben, M. Hemmer, C. D. Schröter, J. Ullrich, T. Pfeifer, et al., *Science* **354**, 308 (2016).

[12] O. L. Krivanek, J. P. Ursin, N. J. Bacon, G. J. Corbin, N. Dellby, P. Hrcicirik, M. F. Murfitt, C. S. Own, and Z. S. Szilagyi, *Philos. Trans. Royal Soc. A* **367**, 3683 (2009).

[13] O. L. Krivanek, T. C. Lovejoy, N. Dellby, T. Aoki, R. W. Carpenter, P. Rez, E. Soignard, J. Zhu, P. E. Batson, M. J. Lagos, et al., *Nature* **514**, 209 (2014).

[14] F. S. Hage, R. J. Nicholls, J. R. Yates, D. G. McCulloch, T. C. Lovejoy, N. Dellby, O. L. Krivanek, K. Refson, and Q. M. Ramasse, *Sci. Adv.* **4**, eaar7495 (2018).

[15] J. A. Hachtel, J. Huang, I. Popovs, S. Jansone-Popova, J. K. Keum, J. Jakowski, T. C. Lovejoy, N. Dellby, O. L. Krivanek, and J. C. Idrobo, *Science* **363**, 525 (2019).

[16] P. E. Batson, N. Dellby, and O. L. Krivanek, *Nature* **418**, 617 (2002).

[17] J. T. van Wijngaarden, E. Verhagen, A. Polman, C. E. Ross, H. J. Lezec, and H. A. Atwater, *Appl. Phys. Lett.* **88**, 221111 (2006).

[18] L. H. G. Tizei and M. Kociak, *Phys. Rev. Lett.* **110**, 153604 (2013).

[19] S. Meuret, L. H. G. Tizei, T. Cazimajou, R. Bourrellier, H. C. Chang, F. Treussart, and M. Kociak, *Phys. Rev. Lett.* **114**, 197401 (2015).

[20] R. Bourrellier, S. Meuret, A. Tararan, O. Stéphan, M. Kociak, L. H. G. Tizei, and A. Zobelli, *Nano Lett.* **16**, 4317 (2016).

[21] M. Kociak and L. F. Zagonel, *Ultramicroscopy* **174**, 50 (2017).

[22] S. Peng, N. J. Schilder, X. Ni, J. van de Groep, M. L. Brongersma, A. Alù, A. B. Khanikaev, H. A. Atwater, and A. Polman, *Phys. Rev. Lett.* **122**, 117401 (2019).

[23] J. Schefold, S. Meuret, N. Schilder, T. Coenen, H. Agrawal, E. C. Garnett, and A. Polman, *ACS Photonics* **4**, 1067 (2019).

[24] S. Vogelgesang, G. Storeck, J. G. Horstmann, T. Diekmann, M. Sivis, S. Schramm, K. Rossnagel, S. Schäfer, and C. Ropers, *NPhy* **14**, 184 (2018).

[25] B. Barwick, D. J. Flannigan, and A. H. Zewail, *Nature* **462**, 902 (2009).

[26] F. J. García de Abajo, A. Asenjo García, and M. Kociak, *Nano Lett.* **10**, 1859 (2010).

[27] S. T. Park, M. Lin, and A. H. Zewail, *New J. Phys.* **12**, 123028 (2010).

[28] S. T. Park and A. H. Zewail, *J. Phys. Chem. A* **116**, 11128 (2012).

[29] F. O. Kirchner, A. Gliserin, F. Krausz, and P. Baum, *Nat. Photon.* **8**, 52 (2014).

[30] L. Piazza, T. T. A. Lummen, E. Quiñonez, Y. Murooka, B. Reed, B. Barwick, and F. Carbone, *Nat. Commun.* **6**, 6407 (2015).

[31] A. Feist, K. E. Echternkamp, J. Schauss, S. V. Yalunin, S. Schäfer, and C. Ropers, *Nature* **521**, 200 (2015).

[32] T. T. A. Lummen, R. J. Lamb, G. Berruto, T. LaGrange, L. D. Negro, F. J. García de Abajo, D. McGrouther, B. Barwick, and F. Carbone, *Nat. Commun.* **7**, 13156 (2016).

[33] K. E. Echternkamp, A. Feist, S. Schäfer, and C. Ropers, *Nat. Phys.* **12**, 1000 (2016).

[34] C. Kealhofer, W. Schneider, D. Ehberger, A. Ryabov, F. Krausz, and P. Baum, *Science* **352**, 429 (2016).

[35] A. Ryabov and P. Baum, *Science* **353**, 374 (2016).

[36] G. M. Vanacore, A. W. P. Fitzpatrick, and A. H. Zewail, *Nano Today* **11**, 228 (2016).

[37] F. J. García de Abajo, B. Barwick, and F. Carbone, *Phys. Rev. B* **94**, 041404(R) (2016).

[38] M. Kozák, J. McNeur, K. J. Leedle, H. Deng, N. Schönenberger, A. Ruehl, I. Hartl, J. S. Harris, R. L. Byer, and P. Hommelhoff, *Nat. Commun.* **8**, 14342 (2017).

[39] A. Feist, N. Bach, T. D. N. Rubiano da Silva, M. Mäller, K. E. Priebe, T. Domräse, J. G. Gatzmann, S. Rost, J. Schauss, S. Strauch, et al., *Ultramicroscopy* **176**, 63 (2017).

[40] K. E. Priebe, C. Rathje, S. V. Yalunin, T. Hohage, A. Feist, S. Schäfer, and C. Ropers, *Nat. Photon.* **11**, 793 (2017).

[41] E. Pomarico, I. Madan, G. Berruto, G. M. Vanacore, K. Wang, I. Kaminer, F. J. García de Abajo, and F. Carbone, *ACS Photonics* **5**, 759 (2018).

[42] G. M. Vanacore, I. Madan, G. Berruto, K. Wang, E. Pomarico, R. J. Lamb, D. McGrouther, I. Kaminer, B. Barwick, F. J. García de Abajo, et al., *Nat. Commun.* **9**, 2694 (2018).

[43] W. Cai, O. Reinhardt, I. Kaminer, and F. J. García de Abajo, *Phys. Rev. B* **98**, 045424 (2018).

[44] Y. Morimoto and P. Baum, *Phys. Rev. A* **97**, 033815 (2018).

[45] Y. Morimoto and P. Baum, *Nat. Phys.* **14**, 252 (2018).

[46] P. Das, J. D. Blazit, M. Tencé, L. F. Zagonel, Y. Auad, Y. H. Lee, X. Y. Ling, A. Losquin, O. S. C. Colliex, F. J. García de Abajo, et al., *Ultramicroscopy* **203**, 44 (2019).

[47] G. M. Vanacore, G. Berruto, I. Madan, E. Pomarico, P. Biagioni, R. J. Lamb, D. McGrouther, O. Reinhardt, I. Kaminer, B. Barwick, et al., *Nat. Mater.* **18**, 573 (2019).

[48] R. Dahan, S. Nehemia, M. Shentcis, O. Reinhardt, Y. Adiv, K. Wang, O. Beer, Y. Kurman, X. Shi, M. H. Lynch, et al., *arXiv* p. 1909.00757 (2019).

[49] O. Kfir, *Phys. Rev. Lett.* **123**, 103602 (2019).

[50] O. Reinhardt, C. Mechel, M. Lynch, and I. Kaminer, *Free-electron qubits* (2019), 1907.10281.

[51] Y. Pan, B. Zhang, and A. Gover, *Phys. Rev. Lett.* **122**, 183204 (2019).

[52] V. Di Giulio, M. Kociak, and F. J. García de Abajo, *Optica* **6**, 1524 (2019).

[53] O. Kfir, H. Lourenço-Martins, G. Storeck, M. Sivis, T. R. Harvey, T. J. Kippenberg, A. Feist, and C. Ropers, *Nature* **582**, 46 (2020).

[54] K. Wang, R. Dahan, M. Shentcis, Y. Kauffmann, A. B. Hayun, O. Reinhardt, S. Tsesses, and I. Kaminer, *Nature* **582**, 50 (2020).

[55] O. Reinhardt and I. Kaminer, *ACS Photonics* **7**, 2859 (2020).

[56] V. Di Giulio and F. J. García de Abajo, p. *arXiv:2008.00957* (2020).

[57] A. Konečná and F. J. García de Abajo, *Phys. Rev. Lett.* **125**, 030801 (2020).

[58] A. Howie, *Microsc. Microanal.* **15**, 314 (2009).

[59] F. J. García de Abajo and M. Kociak, *New J. Phys.* **10**, 073035 (2008).

[60] R. H. Ritchie and A. Howie, *Philos. Mag.* **36**, 463 (1977).

[61] G. Guzzinati, A. Beche, H. Lourenco-Martins, J. Martin, M. Kociak, and J. Verbeeck, *Nat. Commun.* **8**, 14999 (2017).

[62] R. Remez, A. Karnieli, S. Trajtenberg-Mills, N. Shapira, I. Kaminer, Y. Lereah, and A. Arie, *Phys. Rev. Lett.* **123**, 060401 (2019).

[63] Y. Pan and A. Gover, *Phys. Rev. A* **99**, 052107 (2019).

[64] A. Gover and A. Yariv, *Phys. Rev. Lett.* **124**, 064801 (2020).

[65] J. Urata, M. Goldstein, M. F. Kimmitt, A. Naumov, C. Platt, and J. E. Walsh, *Phys. Rev. Lett.* **80**, 516 (1998).

[66] A. Gover, R. Ianconescu, A. Friedman, C. Emma, N. Sudar, P. Musumeci, and C. Pellegrini, *Rev. Mod. Phys.* **91**, 035003 (2019).

[67] H. L. Andrews and C. A. Brau, *Phys. Rev. Spec. Top. AC* **7**, 070701 (2004).

[68] P. Emma, R. Akre, J. Arthur, R. Bionta, C. Bostedt, J. Bozek, A. Brachmann, P. Bucksbaum, R. Coffee, F.-J. Decker, et al., *Nat. Photon.* **4**, 641 (2010).

[69] V. Di Giulio and F. J. García de Abajo, *New J. Phys.* (2020), URL <http://iopscience.iop.org/10.1088/1367-2630/abbddf>.

[70] S. J. Smith and E. M. Purcell, *Phys. Rev.* **92**, 1069 (1953).

[71] P. M. van den Berg, *J. Opt. Soc. Am.* **63**, 1588 (1973).

[72] O. Haeberlé, P. Rullhusen, J. M. Salomé, and N. Maene, *Phys. Rev. E* **55**, 4675 (1997).

[73] J. R. M. Saavedra, D. Castells-Graells, and F. J. García de Abajo, *Phys. Rev. B* **94**, 035418 (2016).

[74] R. Remez, N. Shapira, C. Roques-Carmes, R. Tirole, Y. Yang, Y. Lereah, M. Soljačić, I. Kaminer, and A. Arie, *Phys. Rev. A* **96**, 061801(R) (2017).

[75] U. Fano, *Phys. Rev.* **124**, 1866 (1961).